Analog Assisted Multichannel Digital Post-Correction for Time-Interleaved ADCs

Guanzhong Huang, Chao Yu, *Member*, *IEEE*, and Anding Zhu, *Senior Member*, *IEEE*

***Abstract*—This paper introduces a new digital post-correction technique for calibrating time-interleaved analog-to-digital converters (ADCs). It utilizes one additional sub-ADC to resolve the performance degradation problem near the Nyquist Rate occurred in the conventional multichannel filtering approach. Time skew, gain, offset and bandwidth mismatches as well as the sub-ADC nonlinearities are all included in the proposed model. One group of coefficients extracted in foreground can be applied to any input frequencies in normal operation. An additional analog sub-circuit path is required but the digital part of the implementation becomes much simpler, which ensures that the overall system complexity does not increase. Furthermore, the digital correction structure can reuse the hardware units in time-multiplexing manner for further power and resource savings. A 12-bit, 4-channel, 1GS/s ADC is used to demonstrate the performance of the proposed post-correction.**

***Index Terms*—Digital Post-correction, Multichannel, Time Interleaved, Analog-to-Digital Converter.**

I. Introduction

THE development of advanced digital communication systems continuously drive the demand for high sampling rate of analog-to-digital converters (ADCs). Even if the scaling technology has already considerably improved the speed of transistors, it is still very difficult for single-channel ADCs to achieve satisfactory performance on power efficiency in very high speed operations. In order to overcome this difficulty, time interleaved architecture has been proposed to compromise the die size with the sampling rate, which makes multi-GS/s conversions possible. However, the parallel structure will introduce various types of mismatches such as time skew, gain, offset, sampling bandwidth, as shown in Fig. 1, which degrade the overall linearity [1].

Fortunately, these mismatches can be calibrated with the help of digital circuits. One common way is to extract the mismatch parameters in digital domain and compensate the errors in analog domain [2]. For instance, time skew is calibrated by programmable phase generator in [3], gain and offset by digital-to-analog converters in [4], bandwidth by adjustable sampling switch in [5]. These types of techniques however require the prior information of the ADCs. The other approach is digital post-correction, which is an efficient and flexible option since the integrated digital circuits can perform faster with lower power consumption. Filter bank [6] and multichannel filtering [7] are two of the most popular solutions, but existing methods suffer performance degradation when the input signal frequency approaches the full Nyquist Rate.

This work was funded by the Microelectronic Circuits Centre Ireland (MCCI).

G. Huang and A. Zhu are with the School of Electrical and Electronic Engineering, University College Dublin, Dublin 4, Ireland (e-mail: guanzhong.huang@ucd.ie; anding.zhu@ucd.ie).

C. Yu is with the State Key Laboratory of Millimeter Waves, Southeast University, Nanjing 210096, China (e-mail: chao.yu@seu.edu.cn).

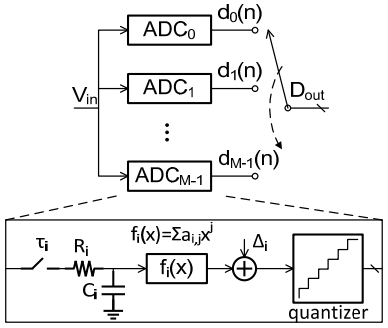

Fig. 1. Structure and error sources of time-interleaved ADC.

To improve the performance, in this work, we propose an analog assisted multichannel digital post-correction technique for time-interleaved ADCs. It is capable of calibrating time skew, gain, offset and bandwidth mismatches as well as the single channel nonlinearity without any knowledge of the ADC structure. By inserting one additional digital sample, captured by using an extra sub-ADC path, in the digital calibration model, this method can effectively correct the mismatches within the whole first Nyquist Zone.

This paper is organized as follows: Section II briefly reviews the conventional multichannel filtering approach and Section III presents the proposed analog assisted multichannel digital post-correction technique. Section IV introduces the model extraction and implementation of the proposed approach. Simulation results are given in Section V, followed by a conclusion in Section VI.

II. Conventional Multichannel Filtering Approach

Different from the filter bank approach [6] where the digital filters take inputs from the corresponding sub-ADC only, multichannel filtering technique [7] utilizes the digital outputs from all sub-ADCs to reconstruct the original signal. Take a 4-channel time-interleaved ADC as an example, the output of i^{th} channel filter $y_i(n)$ can be expressed as:

$$y_i(n) = \sum_{j=-L}^{L} w_i(j)\, d(n-j), \quad i = 1,2,3,4 \qquad (1)$$

where $d(n)$ represents the raw output data with distortion and

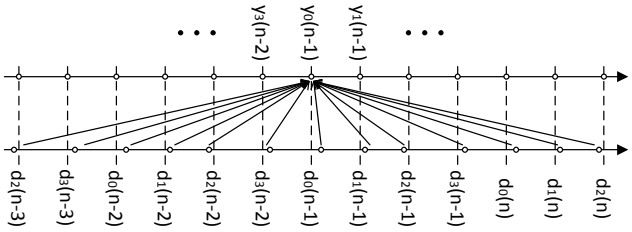

Fig. 2. Signal reconstruction of ADC_0 from an example of 4-channel time-interleaved ADC using multichannel filters.

$w_i(j)$ represents one set of coefficients. In this case, as shown in Fig. 2, the signal reconstruction for ADC_0 will make use of the samples coming from not only its corresponding channel $d_0(n)$, $d_0(n\text{-}1)$, but all the other channels, that is, $d_2(n\text{-}3)$, $d_3(n\text{-}3)$, …, $d_1(n)$, $d_2(n)$. These filters are functioning equivalently to fractional delay filters [6]-[8], which can effectively compensates the time mismatches among the channels. However, like all the other Finite Impulse Response (FIR) filters, the approaches suffer from two drawbacks: firstly, filter length must be large enough to achieve satisfactory performance, which can become a major issue if the number of channels is large; secondly, the finite length of the filters inevitably limits the performance when the input frequency is close to the Nyquist Rate. The survey in [8] has pointed out that almost all the uniform filters, including the FIR filters discussed above, cannot maintain the performance in this region.

III. Proposed Analog Assisted Structure

To resolve the problems mentioned above, in this paper, we propose to use an additional sub-ADC channel to capture a sample from analog domain and then use it in the multichannel digital signal reconstruction. Take a 4-channel time-interleaved ADC as an example again, shown in Fig. 3. Firstly, the digital raw output of each channel is processed by a polynomial component, marked as PLY_i. It fixes the gain, offset mismatch and single channel nonlinearity with the equation expressed as:

$$x_i(n) = \delta_i + \alpha_{i1} d_i(n) + \alpha_{i3} d_i^3(n) \qquad (2)$$

where δ_i and $d_i(n)$ are the offset and the raw digital output of i-th channel respectively while x_i(n) is the output of PLY_i. Different from the conventional multichannel filtering approach, in the new architecture, we add in one digital sample captured from the additional sub-ADC path to calculate the output of multichannel filters ($Filter_i$),

$$y_i(n) = w_i(L+1)\, x_a(n) + \sum_{j=-L}^{L} w_i(j)\, x(n-j) \qquad (3)$$

where $x_a(n)$ is the output of the additional channel and $w_i(L+1)$ is its coefficient while x(n) is output samples from the sub-ADCs and $x(i+M\cdot n)=x_i(n)$, where M is the interleaving factor.

It is worth mentioning that the additional channel is only used to capture additional samples from the analog input. It does not affect the original sampling clock rate. For instance, the sampling rate is still $f_s/4$ but not $f_s/5$. Fig. 4 illustrates the operation. ADC_0 is collecting the consecutive sampled data

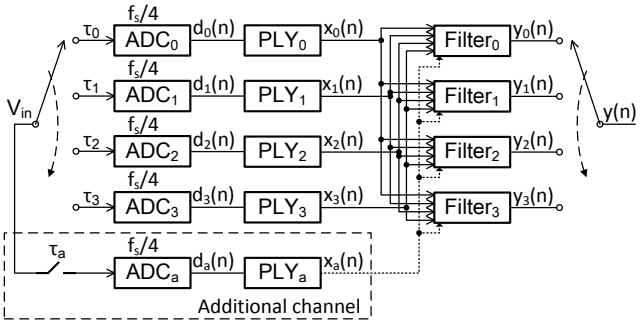

Fig. 3. Structure of the proposed analog assisted digital post-correction for a 4-channel time-interleaved ADC.

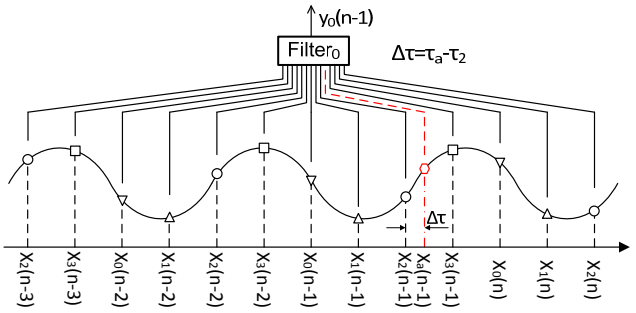

Fig. 4. Input data collection of the post-correction block.

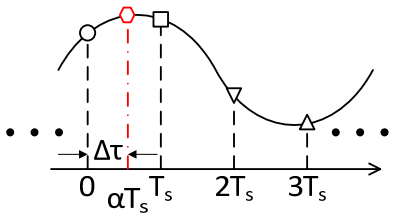

Fig. 5. Non-uniform sampling.

spreading evenly on the two sides of the current sample from normal parallel outputs (ADC_0 – ADC_{M-1}) plus the additional channel (ADC_M) to build up a filter for post-correction, i.e., $y_0(n\text{-}1)=w_0(7)x_a(n\text{-}1)+w_0(6)x_2(n)+w_0(5)x_1(n)+w_0(4)x_0(n)+w_0(3)x_3(n\text{-}1)+w_0(2)x_2(n\text{-}1)+w_0(1)x_1(n\text{-}1)+w_0(0)x_0(n\text{-}1)+w_0(\text{-}1)x_3(n\text{-}2)+w_0(\text{-}2)x_2(n\text{-}2)+w_0(\text{-}3)x_1(n\text{-}2)+w_0(\text{-}4)x_0(n\text{-}2)+w_0(\text{-}5)x_3(n\text{-}3)+w_0(\text{-}6)x_2(n\text{-}3)$. The next channel ADC_1 collects the same source of parallel data plus the most recent sample and minus the oldest one while the additional channel sample stays the same, i.e., $y_1(n\text{-}1)=w_1(7)x_a(n\text{-}1)+w_1(6)x_3(n)+w_1(5)x_2(n)+w_1(4)x_1(n)+w_1(3)x_0(n)+w_1(2)x_3(n\text{-}1)+w_1(1)x_2(n\text{-}1)+w_1(0)x_1(n\text{-}1)+w_1(\text{-}1)x_0(n\text{-}1)+w_1(\text{-}2)x_3(n\text{-}2)+w_1(\text{-}3)x_2(n\text{-}2)+w_1(\text{-}4)x_1(n\text{-}2)+w_1(\text{-}5)x_0(n\text{-}2)+w_1(\text{-}6)x_3(n\text{-}3)$. It continues until the next cycle of ADC_0, $y_0(n)$, that $x_a(n\text{-}1)$ is shifted to $x_a(n)$. Because this digital sample is acquired from the additional path from analog domain, we call the new architecture "analog assisted multichannel digital post-correction".

The idea of using one additional channel for time skew calibration has been published in the literature. For instance, in [3], an additional channel was used as the reference channel to make alignment for each sub-channel. The difference is that the additional channel here is for acquiring an additional digital

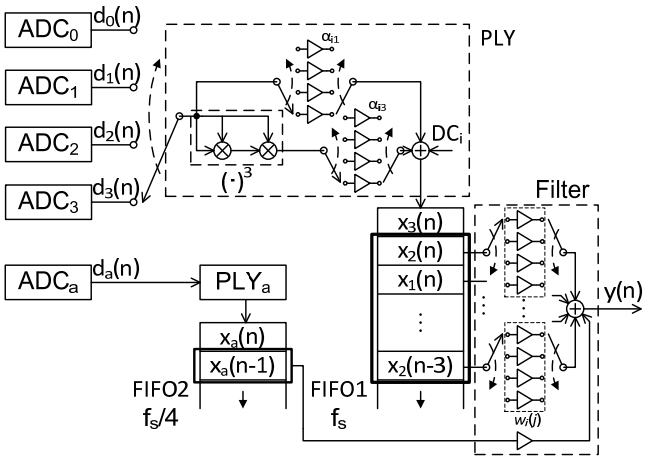

Fig. 6. The proposed post-correction digital implementation for a 4-channel time-interleaved ADC.

sample only. The sampling rate of the additional channel is the same as that of the other channels, i.e., f_s/M, while in [3], the sampling frequency of the additional channel must be carefully assigned in order to make correct correlations between channels. Furthermore, in [3], the rising or falling edge of the clock must be correctly aligned. Here the clock delay between the additional channel and the others can be arbitrarily chosen as long as it does not exactly overlap with any one of the other channels. In the case of Fig. 4, the additional channel uses the sampling clock of ADC_2 with a delay of $\Delta\tau$.

To further explain, the proposed idea is similar to the concept of the non-uniform impulse response representation in [9]. As illustrated in Fig. 5, the conventional multichannel filtering approach is equivalently to take samples uniformly and thus with a finite length of the filter, the capability of signal reconstruction is limited. While in the proposed approach, adding additional sample equivalently makes the multichannel filters become non-uniform format, which makes perfect reconstruction within the Nyquist rate possible [6]. This non-uniform approach also can reduce the length of the digital filters employed. Therefore, although adding an additional sub-ADC channel requires more hardware resource, the total cost of the system may not increase much because the length of the digital filters can be much shorter in the new structure compared to that in the conventional model. Further verification will be given in Section V.

IV. Model Extraction and Implementation

By cascading the polynomial functions and the multichannel filters, the proposed digital post-correction can calibrate all types of mismatches including nonlinearities in each individual channel. The model coefficients can be extracted in foreground and then applied to unknown input signals in normal operation. Digital circuit resource can be reused in the operation to further improve the power efficiency.

A. Coefficients Extraction

Sine waves of different frequencies can be used as input signals for coefficients extraction. With the time-interleaved conversion, the estimated ideal output, $\hat{Y}_{MN\times1}(\omega_{in})$, is calculated by sine wave fitting [10]. ω_{in} is the sine wave input frequency. $\hat{Y}_{MN\times1}(\omega_{in})$, is then de-multiplexed to every sub-ADC, as $\hat{Y}_{0,N\times1}(\omega_{in})$, $\hat{Y}_{1,N\times1}(\omega_{in})$, …, $\hat{Y}_{M\text{-}1,N\times1}(\omega_{in})$. One set of PLY and the filter coefficients of each channel applies for the first Nyquist Zone. The output of PLY_i is calculated as:

$$X_{i,\mathrm{N}\times1} = P_{i,\mathrm{N}\times3}\hat{c}_{pi,3\times1} \tag{4}$$

where

$$P_{i,N\times3} = \begin{bmatrix} 1 & d_i(1) & d_i^3(1) \\ 1 & d_i(2) & d_i^3(2) \\ \vdots & \vdots & \vdots \\ 1 & d_i(N) & d_i^3(N) \end{bmatrix}, \hat{c}_{pi} = \begin{bmatrix} \delta_i \\ \alpha_{i1} \\ \alpha_{i3} \end{bmatrix} \tag{5}$$

A set of sine waves with different frequencies, ω_1, ω_2, …, ω_K, spread over the Nyquist Rate serve as the input signal for calibration. By using Least Square (LS), the estimated coefficients of PLY_i can be expressed as:

$$\hat{c}_{pi,3\times1} = \left(\tilde{P}_{i,3\times KN}^H \tilde{P}_{\mathrm{KN}\times3}\right)^{-1} \tilde{P}_{i,3\times KN}^H \tilde{Y}_{i,\mathrm{KN}\times1} \tag{6}$$

where

$$\tilde{P}_{i,\mathrm{KN}\times3} = \begin{bmatrix} P_{i,\mathrm{N}\times3}(\omega_1) \\ P_{i,\mathrm{N}\times3}(\omega_2) \\ \vdots \\ P_{i,\mathrm{N}\times3}(\omega_K) \end{bmatrix}, \tilde{Y}_{i,\mathrm{KN}\times1} = \begin{bmatrix} \hat{Y}_{i,\mathrm{N}\times1}(\omega_1) \\ \hat{Y}_{i,\mathrm{N}\times1}(\omega_2) \\ \vdots \\ \hat{Y}_{i,\mathrm{N}\times1}(\omega_K) \end{bmatrix} \tag{7}$$

The output of $Filter_i$ can be expressed as

$$Y_{i,N\times1} = F_{i,N\times(2L+2)}\hat{c}_{fi,(2L+2)\times1} \tag{8}$$

where

$$F_{i,N\times(2L+2)} = \begin{bmatrix} x_M(1) & \cdots & x_i(1) & \cdots \\ \vdots & & \vdots & \vdots \\ x_M(n) & \cdots & x_i(n) & \cdots \\ \vdots & & \vdots & \vdots \\ x_M(N) & \cdots & x_i(N) & \cdots \end{bmatrix}$$

$$\hat{c}_{fi} = \begin{bmatrix} w_i(L+1) & w_i(L) & \cdots & w_i(0) & \cdots & w_i(-L) \end{bmatrix}^T \tag{9}$$

With the PLY array outputs, the coefficients of $Filter_i$ can be estimated from:

$$\hat{c}_{fi,(2L+2)\times1} = \left(\tilde{F}_{i,(2L+2)\times KN}^H \tilde{F}_{KN\times(2L+2)}\right)^{-1} \tilde{F}_{i,(2L+2)\times KN}^H \hat{Y}_{i,KN\times1} \tag{10}$$

where

$$\tilde{F}_{i,\mathrm{KN}\times(2L+2)} = \begin{bmatrix} F_{i,\mathrm{N}\times(2L+2)}(\omega_1) \\ F_{i,\mathrm{N}\times(2L+2)}(\omega_2) \\ \vdots \\ F_{i,\mathrm{N}\times(2L+2)}(\omega_K) \end{bmatrix} \tag{11}$$

After obtaining $\hat{c}_{pi}$ and $\hat{c}_{fi}$ for each channel, the time-interleaved ADC is then able to achieve good linearity after post-correction with (4) and (8) in cascade for any input within the Nyquist Rate.

B. Digital Circuits Implementation

The PLY functions and the multichannel filters at different channels use the same structure and they are not necessarily operated at the same time. It makes digital hardware reusable,

TABLE I
MISMATCH AND NONLINEARITY PARAMETERS

No.	τ_i (ps)	g_i	δ_i/FS	R_{on} (Ω)	Nonlinearity	
					2nd order	3rd order
0	5	0.9337	3.219×10^{-3}	100	0.0066	-0.0058
1	-15	1.052	-9.866×10^{-3}	101	-0.0003	-0.011
2	17	0.9843	8.229×10^{-3}	98	-0.0067	-0.0056
3	-22	1.015	-7.167×10^{-3}	103	-0.0016	0.0053
4*	-2	0.9712	-1.239×10^{-3}	102	0.0023	-0.0077

* Additional channel.

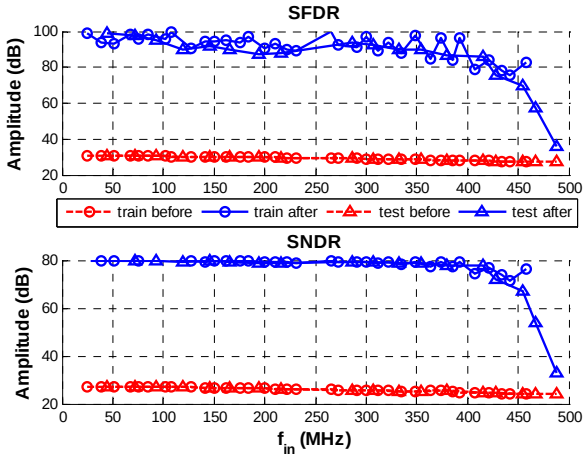

Fig. 7. SFDR/SNDR before and after post-correction using the conventional approach.

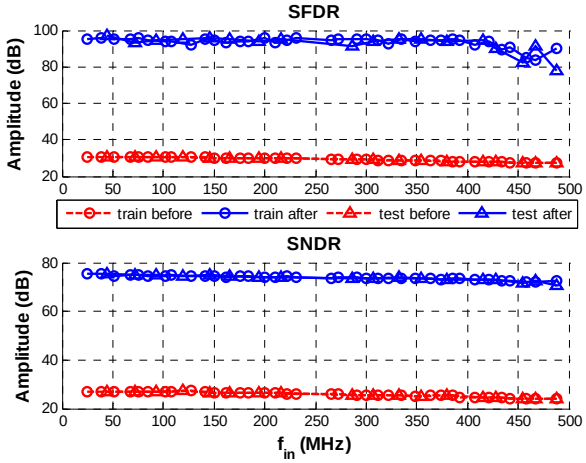

Fig. 8. SFDR/SNDR before and after post correction using the proposed approach.

as shown in Fig. 6. One set of PLY and the filter running in f_s is enough for four channels with four different sets of coefficients switched in time-multiplexing manner. Two First-In-First-Outs (FIFOs), which are depicted in the bold lined boxes, operate as buffers between PLY and the filter array. With the switches set to the state in Fig. 6, the multichannel filter generates the corrected output of ADC_0, $y_0(n\text{-}1)$. The detailed expression is given in the last section. In the next clock cycle, the data in FIFO1 shift to $\{x_3(n), x_2(n), x_1(n), x_0(n), x_3(n\text{-}1), x_2(n\text{-}1), x_1(n\text{-}1), x_0(n\text{-}1), x_3(n\text{-}2), x_2(n\text{-}2), x_1(n\text{-}2), x_0(n\text{-}2), x_3(n\text{-}3)\}$ while FIFO2 stays the same. It corresponds to the corrected output of ADC_1, $y_1(n\text{-}1)$. After another three cycles, the data in FIFO2 will shift

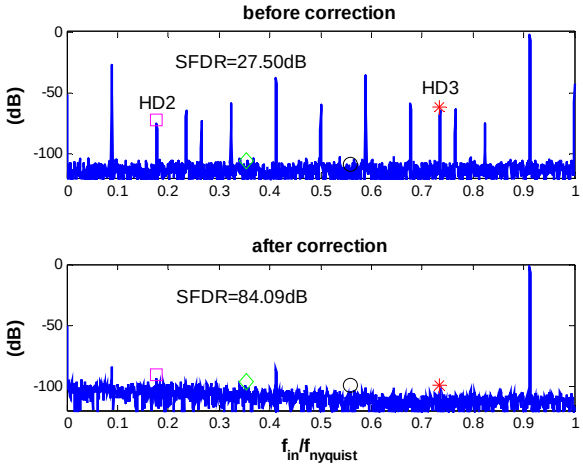

Fig. 9. Spectrum plot of the single-tone test.

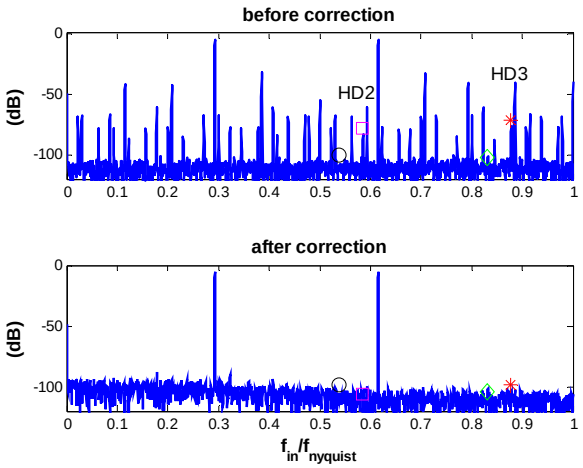

Fig. 10. Spectrum plot of the two-tone test.

to $\{x_d(n\text{-}1)\}$. As a result, FIFO1 runs at f_s and FIFO2 at $f_s/4$. The number of multipliers is reduced to 1/4. The additional channel needs another set, but it runs at $f_s/4$.

V. SIMULATION RESULTS

The simulation is built up with four types of mismatches and nonlinearities in single channels. The first order RC network is used to model the sampling bandwidth mismatch of each channel. The frequency response can be expressed as:

$$H_i(\omega) = \frac{1}{1 + j\omega R_i C_i} \tag{12}$$

where R_i and C_i is the on-resistance and sampling capacitance of the i-th channel. As a result, the equivalent time skew and gain mismatches introduced by bandwidth mismatch are both input frequency dependent.

The mismatch and nonlinearity parameters of a 12-bit, 4-channel, 1GS/s time interleaved ADC are given in TABLE I. The Sampling capacitance of each channel is set to be a constant since the mismatch of on-resistance dominates their product. For comparison, we employ the conventional multichannel filters to calibrate the distortion first. The performance of spurious free dynamic range (SFDR) and signal

TABLE II
NUMBER OF COEFFICIENTS COMPARISON

	PLY	Filter
Multichannel filters	3×4	45×4
The proposed	3×5	22×4

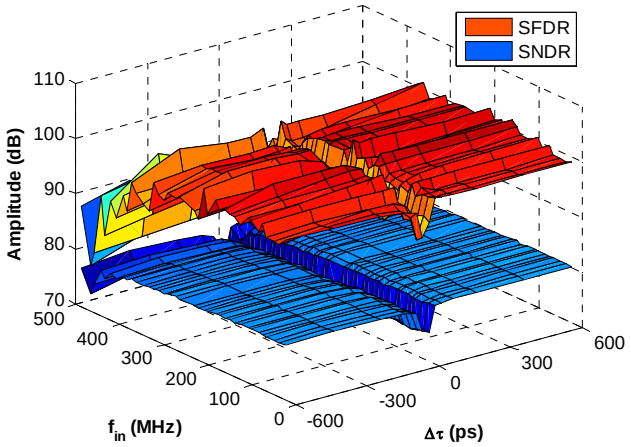

Fig. 11. Correction performance vs. delay time of the additional channel.

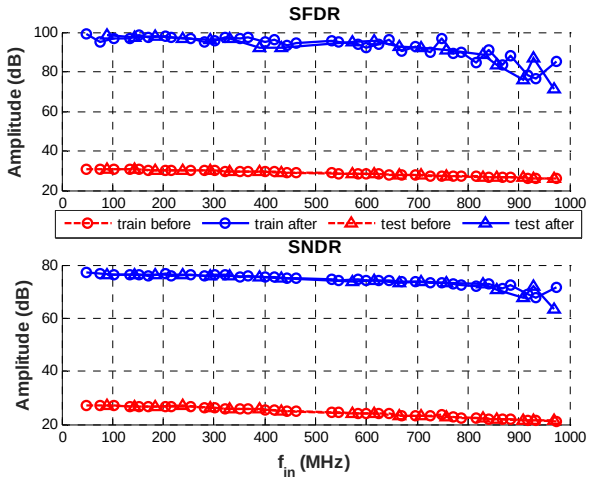

Fig. 12. SFDR/SNDR before and after post-correction an 8-channel time interleaved ADC.

to noise and distortion ratio (SNDR) between before and after post-correction is shown in Fig. 7. The "training" points, depicted as circles, representing the frequency points that are used for coefficients extraction; the "test" points, depicted as triangles, are the arbitrary input frequencies. As explained in Section II, the performance degrades when f_{in} approaches the Nyquist Rate. If the training frequencies range from 0 to $0.9*f_{nyquist}$, as shown in Fig. 7, the calibrated performance is good within this region but drop dramatically when f_{in} is over $0.9*f_{nyquist}$. On the other hand, if the training frequencies cover the first Nyquist Zone, it will smooth the degradation around $f_s/2$, but the overall performance is compromised by around 5dB when $f_{in}<f_s/4$ and more than 10dB when $f_{in}>f_s/4$. After the additional channel is used, the performance can be significantly improved, as shown in Fig. 8. Spectrum plots of the single-tone and two-tone tests are given in Fig. 9 and Fig. 10, respectively.

As mentioned earlier, there is no particular requirement for the additional sub-ADC path on the delay, e.g., Δτ, in Fig. 4, as long as it does not overlap with the other channels. This can be seen from the results shown in Fig. 11. The proposed method also works for larger number of interleaving. An 8-channel ADC with the same sub-channel speed and mismatch level is corrected to good performance as shown in Fig. 12. In this case, the overhead of extra channel becomes smaller.

About complexity of the digital part, the number of coefficients is smaller because the filter length is smaller compared to that in the conventional approach. For example, in this test, to achieve the same performance, 45 coefficients are required in the conventional model while only 22 coefficients for the proposed model, as given in TABLE II.

VI. CONCLUSION

By adding an additional sub-ADC channel, the proposed multichannel post-correction can maintain the calibration performance in the full Nyquist Rate. It also consumes less resource in digital domain when achieving the same performance, compared to the conventional multichannel filters approach. Reusing digital hardware can further save resources. Simulation results demonstrated that excellent calibration performance can be achieved by employing the proposed approach.

REFERENCES

[1] N. Kurosawa, H. Kobayashi, *et al.*, "Explicit analysis of channel mismatch effects in time-interleaved ADC systems," *IEEE Trans. Circuits and Syst. I*, vol. 48, no. 3, pp. 261–271, 2001.
[2] B. Razavi, "Problem of timing mismatch in interleaved ADCs," *IEEE Custom Integrated Circuits Conf.*, pp. 1–8, San Jose, CA, Sep. 2012.
[3] M. El-Chammas and B. Murmann, "A 12-GS/s 81-mW 5-bit time-interleaved flash ADC with background timing skew calibration," *IEEE J. Solid-State Circuits*, vol. 46, no. 4, pp. 838–847, 2011.
[4] Y. M. Greshishchev, J. Aguirre, *et al.*, "A 40GS/s 6b ADC in 65nm CMOS," *ISSCC Dig. Tech. Papers*, pp. 390-391, 2010.
[5] R. Payne, C. Sestok, *et al.*, "A 12b 1GS/s SiGe BiCMOS two-way time-interleaved pipeline ADC," *ISSCC Dig. Tech. Papers*, pp. 182-184, 2011.
[6] H. Johansson and P. Lowenborg, "Reconstruction of nonuniformly sampled bandlimited signals by means of digital fractional delay filters," *IEEE Trans. Signal Processing*, vol. 50, no. 11, pp. 2757–2767, 2002.
[7] Y. C. Lim, Y.-X. Zou, *et al.*, "Time-interleaved analog-to-digital converter compensation using multichannel filters," *IEEE Trans. Circuits and Syst. I*, vol. 56, no. 10, pp. 2234–2247, 2009.
[8] T. I. Laakso, V. Valimaki, *et al.*, "Splitting the unit delay [FIR/all pass filters design]," *IEEE Signal Processing Magazine*, vol. 13, no. 1, pp. 30–60, 1996.
[9] T. J. Brazil, "Accurate and efficient incorporation of frequency-domain data within linear and non-linear time-domain transient simulation," *IEEE MTT-S Int. Micro. Symp. Dig.*, 2005.
[10] P. Handel, "Properties of the IEEE-STD-1057 four-parameter sine wave fit algorithm," *IEEE Trans. Instrumentation and Measurement*, vol. 49, no. 6, pp. 1189–1193, 2000.